

Locally Private Graph Neural Networks

Sina Sajadmanesh
sajadmanesh@idiap.ch
Idiap Research Institute, EPFL

Daniel Gatic-Perez
gatica@idiap.ch
Idiap Research Institute, EPFL

ABSTRACT

Graph Neural Networks (GNNs) have demonstrated superior performance in learning graph representations for several subsequent downstream inference tasks. However, learning over graph data can raise privacy concerns when nodes represent people or human-related variables that involve personal information about individuals. Previous works have presented various techniques for privacy-preserving deep learning over non-relational data, such as image, audio, video, and text, but there is less work addressing the privacy issues involved in applying deep learning algorithms on graphs. As a result and for the first time, in this paper, we develop a privacy-preserving GNN learning algorithm with formal privacy guarantees based on Local Differential Privacy (LDP) to tackle the problem of node-level privacy, where graph nodes have potentially sensitive features that need to be kept private, but they could be beneficial for an untrusted server to learn richer node representations. Specifically, we propose an optimized LDP algorithm with an unbiased estimator, using which a central server can communicate with the graph nodes to privately collect their data and estimate the graph convolution layer of the GNN. To further reduce the effect of the injected noise, we propose a simple graph convolution layer based on the multi-hop aggregation of the nodes' features. Extensive experiments conducted over real-world datasets demonstrate the capability of our method in maintaining an appropriate privacy-accuracy trade-off for privacy-preserving node classification.

1 INTRODUCTION

Following the advances of deep neural networks in various machine learning domains, such as computer vision, natural language understanding, and speech processing, in the past few years, extending deep learning models for graph-structured data has attracted growing interest, leading to the advent of Graph Neural Networks (GNNs) [36]. GNNs have shown superior performance in a wide range of applications in social sciences [13], biology [32], molecular chemistry [9], and so on, achieving state-of-the-art results in various graph-based learning tasks, such as node classification [21], link prediction [46], and community detection [6]. However, most real-world graphs associated with people or human-related activities, such as social and economic networks, are often sensitive and contain personal information. For example in a social network, a user's friend list, profile information, likes and comments, etc., could potentially be private to the user. To satisfy users' privacy expectations in accordance with the recent legal data protection policies, such as European General Data Protection Regulations (GDPR), it is of great importance to develop privacy-preserving GNN models for applications that rely on graphs accessing users' personal data.

Problem and motivation. In light of these privacy considerations and (to our knowledge) for the first time, we define the

problem of node-level privacy, where graph nodes have potentially sensitive attributes that are kept private, but the topology of the graph is observable from the viewpoint of a central server, who wishes to benefit from private node attributes to learn a GNN over the graph. The ability to learn graph representations from private node features is useful in many applications in social network analysis and mobile computing. For example, a social smartphone application server (e.g., social networks, messaging platforms, and dating apps), which is using a GNN as part of its recommendation system [11], could potentially benefit from users' personal information, such as their phone's sensor data or list of installed apps, by incorporating them into their GNN model to learn better user representations, leading to improved quality of service. However, without any means of data protection, this implies that the server needs to get access to and collect personal raw data, which can raise privacy concerns as the collected data can be used for other, unauthorized purposes.

Challenges. Training a GNN under the node-level privacy setting is challenging due to the relational characteristics of graphs. Unlike other deep learning models wherein the training data are independent, in the case of GNNs, the samples – nodes of the graph – are connected to each other via links and exchange information through a message-passing framework during training [14]. This fact renders common privacy-preserving machine learning paradigms, such as federated and split learning [18, 29, 49], infeasible due to their excessive communication overhead. This is because in the absence of a trusted server, which is the main assumption of our paper, every adjacent pair of nodes have to exchange their embeddings with each other multiple times during a single epoch, which is much higher communication than the case for conventional deep neural networks, where the nodes only communicate with the server. Besides, our problem is different from and more challenging than differentially private model publishing, where the data is completely accessible by the server, and the aim is to train and then publish a model in a way that the released model does not expose information about the training data, which is typically done by adding differentially private noise to the gradients of the model during training [2], or training the model using a noisy loss function [48]. In our problem setting, however, the server is not trusted and thus does not have direct access to the data (node features), and accordingly, an extra layer of protection should be implemented between the user's data and the server.

Contributions. In this paper, we propose a novel privacy preserving GNN learning framework with provable privacy guarantees based on Local Differential Privacy (LDP) [19] to protect sensitive node attributes from being exposed to an honest-but-curious server [31], who requires these features for training a GNN. The key idea behind our method is to exploit the fact that node features are first aggregated in the initial layer of the GNN before getting

passed to the non-linear activation function. Therefore, it allows to inject a differentially private noise into the node features that would be averaged out during the neighborhood aggregation in the first layer of the GNN. To this end, we propose an optimized LDP mechanism, using which the server can efficiently communicate with the graph nodes to privately collect their features with minimum communication overhead. We then design an unbiased estimator to estimate the first layer neighborhood aggregation from the collected node features. Additionally, we employ a simple, yet effective graph convolution layer based on the multi-hop aggregation of the nodes’ features to increase the estimation accuracy for the low-degree nodes. We derive the theoretical properties of the proposed algorithm, such as its formal privacy guarantee and error bound. Finally, we conduct comprehensive experiments over several real-world datasets to demonstrate that the proposed GNN is robust to the injected LDP noise for the privacy-preserving node classification task. To the best of our knowledge, this paper defines the problem of learning GNN with node-level privacy for the first time, studying the integration of differential privacy with GNNs.

Paper organization. The rest of this paper is organized as follows. In Section 2, we formally define the problem and provide the necessary backgrounds. Then, in Section 3, we introduce our privacy-preserving GNN training algorithm. Details of experiments and their results are explained in Section 4. We discuss the proposed method and review the related work in Section 5 and Section 6, respectively. Finally, we conclude the paper in Section 7. The proofs of all the theoretical findings are also presented in Appendix A.

2 PRELIMINARIES

Problem definition. We formally define the problem of training a GNN under the node-level privacy setting. Assume that an honest-but-curious server has access to a graph $\mathcal{G} = (\mathcal{V}, \mathcal{E}, \mathbf{X})$, whose node set \mathcal{V} and link set \mathcal{E} are visible by the server, but the feature matrix $\mathbf{X} \in \mathbb{R}^{|\mathcal{V}| \times d}$, comprising d -dimensional feature vectors \mathbf{x}_v for each node $v \in \mathcal{V}$, is private to the nodes and thus not observable by the server. The problem is: how can the server collaborate with the nodes to train a GNN over \mathcal{G} without letting the private features leave the nodes? To answer this question, we first present the required background about local differential privacy and GNNs.

Local Differential Privacy. Local differential privacy (LDP) is an increasingly used approach for collecting private data and computing statistical queries, such as mean, count, and histogram, and is already deployed by Google, Apple, and Microsoft for private data analytics at scale [44]. The key idea behind LDP is that data holders do not need to share their private data with a data aggregator, but instead send a perturbed version of their data, which is not meaningful individually but can approximate the target query when aggregated. It includes two steps: (i) data collection, in which each data holder perturbs its data using a special randomized mechanism \mathcal{M} and sends the output to the aggregator; and (ii) estimation, in which, the aggregator combines all the received perturbed values and estimates the target query. To prevent the aggregator from inferring the original private value from the perturbed one, the mechanism \mathcal{M} must satisfy the following definition [19]:

Definition 2.1. Given $\epsilon > 0$, a randomized mechanism \mathcal{M} satisfies ϵ -local differential privacy, if for all possible pairs of user’s private data x and x' , and for all possible outputs $y \in \text{Range}(\mathcal{M})$, we have:

$$\Pr[\mathcal{M}(x) = y] \leq e^\epsilon \Pr[\mathcal{M}(x') = y] \quad (1)$$

The parameter ϵ in the above definition is called the “*privacy budget*” and is used to tune utility versus privacy: a smaller (resp. larger) ϵ leads to stronger (weaker) privacy guarantees, but lower (higher) utility. The above definition implies that the mechanism \mathcal{M} should assign similar probabilities (controlled by ϵ) to the outputs of different input values x and x' , so that by looking at the outputs, an adversary could not infer the input value with high probability, regardless of any side knowledge they might have. LDP is achieved for a deterministic function usually by adding a special noise to its output that would cancel out in calculating the target aggregation having a sufficiently large number of noisy samples.

Graph Neural Networks. A GNN learns the representation of a node by iteratively aggregating the embeddings of its adjacent neighbors followed by a non-linear transformation. More formally, Given a graph $\mathcal{G} = (\mathcal{V}, \mathcal{E}, \mathbf{X})$, a L -layer GNN consists of L graph convolution layers, where the embedding h_v^l of a node $v \in \mathcal{V}$ at layer l is generated by aggregating the previous layer’s embeddings of its neighbors through the neighborhood aggregation step, as:

$$h_{\mathcal{N}(v)}^l = \text{AGGREGATE}_l \left(\{h_u^{l-1}, \forall u \in \mathcal{N}(v)\} \right) \quad (2)$$

$$h_v^l = \sigma \left(\mathbf{W}_l \cdot h_{\mathcal{N}(v)}^l \right) \quad (3)$$

where $\mathcal{N}(v)$ is the set of neighbors of v including itself and h_u^{l-1} is the embedding of node u at layer $l - 1$. AGGREGATE_l and $h_{\mathcal{N}(v)}^l$ are respectively the l -th layer differentiable, permutation invariant aggregator function (such as mean, sum, or max) and its output on $\mathcal{N}(v)$. Finally, \mathbf{W}^l is the trainable weight matrix for layer l , and σ is a non-linear activation function (e.g. a ReLU). Here, $h_v^0 = \mathbf{x}_v$, i.e., the initial embedding of v is its feature vector \mathbf{x}_v .

3 PROPOSED METHOD

Now, we describe our proposed framework for learning a GNN using private node features. As we have seen in the previous section, in the forward propagation of a GNN, the node features are firstly aggregated in the initial layer prior to applying the non-linear transformation. This is an advantage from a privacy-preserving perspective, because it allows to use an LDP mechanism to perturb the input features, and then let the first-layer’s aggregator function average out the injected noise (to an extent), yielding a (relatively) noise-free, statistically unbiased embedding for the subsequent layer. This is, however, provided that the aggregator function be *linear* in the node features (e.g., mean or sum), which is hopefully the case for many popular GNN variants, such as Graph Convolutional Networks (GCNs) [21]. As a result, the foundation of our proposed algorithm is to use an LDP mechanism to obfuscate the nodes’ features, which are then collected by the server. Having once stored the privately collected features, the server does not need to get back to the nodes again and can train the locally private GNN with minimum communication.

However, maintaining a proper balance between the accuracy of the GNN and the privacy of data is a challenging task, which needs to be addressed carefully. On the one hand, the node features to be collected are likely multidimensional, so the perturbation of every single feature consumes privacy budget. If we want to keep our total budget ϵ low to provide better privacy protection, we need to perturb each of the d features with ϵ/d budget (because the privacy budgets of the features add up together as the result of the composition theorem [10]), which in turn results in adding more noise to the data that can significantly degrade the final accuracy. On the other hand, in order for the GNN to be able to cancel out the injected noise, the first layer’s aggregator function needs to be calculated over a sufficiently large set of node features. However, in many real-world graphs, which usually have Power-Law degree distribution, the number of low-degree nodes are much more than the high-degree ones. For instance, the mean degree of the famous Cora dataset [45] is only about 4. With such a low degree, the estimated aggregation would most likely be very noisy, again leading to noticeable performance loss.

In order to tackle the first challenge, we develop an optimized multidimensional LDP method, called the *multi-bit mechanism*, by extending the 1-bit mechanism [7] for multidimensional feature collection. Our mechanism is designed for communication efficiency, and we show that it works better than the commonly used Gaussian mechanism [10]. For the second challenge, we propose a simple, yet effective graph convolution layer, called *KProp*, which aggregates messages from an expanded neighborhood set that includes both the immediate neighbors and those nodes that are up to K -hops away. In the experiments, we show that this technique can boost the performance of our locally private GNN, especially for graphs with lower average degree.

3.1 Collection of node features

Algorithm 1 describes our multi-bit mechanism for privately collecting node features. Assume that each node v owns a private d -dimensional feature vector x_v whose elements lie in the range $[\alpha, \beta]$. When the feature vector of v is requested by the server, the node locally applies the multi-bit mechanism on x_v to get the corresponding perturbed feature vector x_v^* , which is then sent back to the server instead of the private vector x_v . The data collection happens only once and before the training, so x_v^* is generated once and is recorded by the node to be returned in subsequent calls, to prevent guessing the private features using repeated queries.

Intuitively, instead of perturbing all the d features, the algorithm first uniformly samples m out of d features without replacement, where m is a parameter controlling how many features are perturbed. Then, for each sampled feature, a corresponding Bernoulli variable is drawn from the distribution indicated in Line 4 of the algorithm, whose parameter depends on the value of the feature and the privacy budget provided by the server. Finally, the output is transformed to be either -1 or 1. For other features which are not perturbed, the algorithm simply outputs 0. Therefore, a maximum of two bits per feature is enough to send x_v^* to the server. When $m = d$, our algorithm reduces to applying the 1-bit mechanism with a privacy budget of ϵ/d to every single feature. The following theorem ensures that the multi-bit mechanism is ϵ -LDP.

Algorithm 1: Multi-Bit Mechanism

Input : feature vector $x \in [\alpha, \beta]^d$; privacy budget $\epsilon > 0$; range parameters α and β ; sampling parameter $m \in \{1, 2, \dots, d\}$.
Output : perturbed vector $x^* \in \{-1, 0, 1\}^d$.
 1 Let S be a set of m values drawn uniformly at random without replacement from $\{1, 2, \dots, d\}$
 2 **for** $i \in \{1, 2, \dots, d\}$ **do**
 3 $s_i = 1$ if $i \in S$ otherwise $s_i = 0$
 4 $t_i \sim \text{Bernoulli}\left(\frac{1}{e^{\epsilon/m+1}} + \frac{x_i - \alpha}{\beta - \alpha} \cdot \frac{e^{\epsilon/m-1}}{e^{\epsilon/m+1}}\right)$
 5 $x_i^* = s_i \cdot (2t_i - 1)$
 6 **end**
 7 **return** $x^* = [x_1^*, \dots, x_d^*]^T$

THEOREM 3.1. *The multi-bit mechanism presented in Algorithm 1 satisfies ϵ -local differential privacy.*

3.2 Approximation of graph convolution

Upon collecting the perturbed data, the server initiates the training of the GNN. In the first layer of the GNN, the embedding for an arbitrary node v is generated by the following, where layer indicator subscripts and superscripts are omitted for simplicity:

$$x'_u = \frac{d(\beta - \alpha)}{2m} \cdot \frac{e^{\epsilon/m} + 1}{e^{\epsilon/m} - 1} \cdot x_u^* + \frac{\alpha + \beta}{2} \quad (4)$$

$$\widehat{h}_{N(v)} = \text{AGGREGATE}(\{x'_u, \forall u \in N(v)\}) \quad (5)$$

$$h_v = \sigma(W \cdot \widehat{h}_{N(v)}) \quad (6)$$

where x'_u is an unbiased estimation for the corresponding private feature vector x_u , and $\widehat{h}_{N(v)}$ is the estimated neighborhood aggregation under LDP. After this step, the server can proceed with the rest of the layers to complete the forward and backward propagation of the model, exactly similar to a standard GNN. The following results follow from our algorithm:

PROPOSITION 3.2. *The estimator defined by (4) is unbiased.*

COROLLARY 3.3. *Given a linear aggregator function, the aggregation defined by (5) is an unbiased estimation for (2) in layer $l = 1$.*

PROPOSITION 3.4. *For any node v and any dimension $i \in \{1, 2, \dots, d\}$, the variance of the unbiased feature estimator defined by (4) is:*

$$\text{Var}[x'_{v,i}] = \frac{d}{m} \cdot \left(\frac{\beta - \alpha}{2} \cdot \frac{e^{\epsilon/m} + 1}{e^{\epsilon/m} - 1} \right)^2 - \left(x_{v,i} - \frac{\alpha + \beta}{2} \right)^2 \quad (7)$$

The variance of an LDP mechanism is the key factor affecting the utility of the estimator. A lower variance usually leads to a more accurate estimation. Therefore, we exploit the result of Proposition 3.4 to find the optimal sampling parameter m in Algorithm 1 that minimizes the variance of the estimator, as follows:

PROPOSITION 3.5. *The optimal value of the sampling parameter m in Algorithm 1, denoted by m^* , is obtained as:*

$$m^* = \max(1, \min(d, \lfloor \frac{\epsilon}{2.18} \rfloor)) \quad (8)$$

3.3 Neighborhood expansion

The neighborhood aggregation estimator defined by (5) estimates the first layer aggregation of any node v by aggregating noisy features of all the nodes adjacent to v . The following proposition shows

Algorithm 2: KProp Convolution Layer

Input : Graph $\mathcal{G} = (\mathcal{V}, \mathcal{E}, X)$; weight matrix W ; linear aggregator function AGGREGATE; step parameter $K \geq 1$; non-linearity σ ;
Output : embedding vector $h_v, \forall v \in \mathcal{V}$

- 1 **for all** $v \in \mathcal{V}$ **do in parallel**
- 2 $h_{\mathcal{N}(v)}^0 = x_v$
- 3 **for** $k = 1$ **to** K **do**
- 4 $h_{\mathcal{N}(v)}^k = \text{AGGREGATE}(\{h_{\mathcal{N}(u)}^{k-1}, \forall u \in \mathcal{N}(v) - \{v\}\})$
- 5 **end**
- 6 $h_v = \sigma(W \cdot h_{\mathcal{N}(v)}^K)$
- 7 **endfor**
- 8 **return** $\{h_v, \forall v \in \mathcal{V}\}$

the relationship of the estimation error and the neighborhood size $|\mathcal{N}(v)|$ for the special case of using the mean aggregator function:

PROPOSITION 3.6. *Given the mean aggregator function for the first layer, with probability at least $1 - \delta$, for any node v , we have:*

$$\max_{i \in \{1, \dots, d\}} \left| (\widehat{h}_{\mathcal{N}(v)})_i - (h_{\mathcal{N}(v)})_i \right| = \mathcal{O} \left(\frac{\sqrt{d \log(d/\delta)}}{\epsilon \sqrt{|\mathcal{N}(v)|}} \right) \quad (9)$$

The above proposition indicates that with the mean aggregator function, the estimation error decreases with a rate proportional to $\sqrt{|\mathcal{N}(v)|}$. Simply speaking, the higher number of neighbors, the lower the estimation error. But as mentioned earlier, the size of $\mathcal{N}(v)$ is usually small in real graphs, which hinders the aggregator to eliminate the effect of the injected noise.

In a different context, prior works have shown that considering higher-order neighbors can be useful in learning better node representations [4, 24, 30]. Inspired by these works, a potential solution to our problem is to expand the neighborhood of each node v by considering more nodes that are not necessarily adjacent to v , but reside within an adjustable local neighborhood around v . To this end, we use an efficient neighborhood aggregation and convolution layer, described in Algorithm 2, that can effectively be used to address the small-size neighborhood issue. The idea is simple: we aggregate features of those nodes that are up to K steps away from v , by simply performing K consecutive neighborhood aggregations, with feature transformation and non-linearity applied only after the K -th aggregation step. For simplicity, we call this algorithm KProp, as every node propagates its message to K hops further. By controlling the parameter K , we can expand the effective aggregation set size for each node. However, it is important to note that we cannot arbitrarily increase the neighborhood size around a node, since aggregating messages from nodes that are too far away could lead to some problems in GNNs such as synchronization and over-smoothing [28]. Therefore, there is a trade-off between the estimation accuracy and the GNN expressive power.

Note that in KProp, we perform aggregations over $\mathcal{N}(v) - \{v\}$, i.e., we do not include self-loops. While it has been shown that adding self-loops can improve accuracy in conventional GNNs [21], we empirically show that excluding self-connections works better when dealing with noisy features. This is because as K grows, with self-loops, we account for the injected noise in the feature vector of each node in the v 's neighborhood multiple times in the aggregation, and thus removing self-loops helps to reduce the total noise by discarding repetitive node features from the aggregation. As a

Algorithm 3: Locally Private GNN Training

Input : Graph $\mathcal{G} = (\mathcal{V}, \mathcal{E})$; depth L ; KProp parameter $K \geq 1$; number of epochs N_e ; privacy budget $\epsilon > 0$; range parameters α and β
Output : Trained GNN weights $\{W^l, \forall l \in \{1, 2, \dots, L\}\}$

- 1 **Server-side:**
- 2 Send ϵ, α, β to every node $v \in \mathcal{V}$.
- 3 **Node-side:**
- 4 Send a perturbed vector x^* using Algorithm 1 to the server.
- 5 **Server-side:**
- 6 **for** $epoch = 1$ **to** N_e **do**
- 7 Obtain x'_v using (4) for all $v \in \mathcal{V}$.
- 8 Obtain h'_v using Algorithm 2 with $\{x'_v, \forall v \in \mathcal{V}\}$.
- 9 **for** $l = 2$ **to** L **do**
- 10 Obtain h'_v using (3) for all $v \in \mathcal{V}$.
- 11 **end**
- 12 Calculate loss, backpropagate, and update W^l for every layer l .
- 13 **end**
- 14 **return** $\{W^l, \forall l \in \{1, 2, \dots, L\}\}$

result, the KProp layer can be seen as an adaptation of the Simple Graph Convolution [40], but without using self-loops and a general aggregator function with the aim of increasing the estimation accuracy of the neighborhood aggregation under differentially private noise. Also, the KProp layer is similar to the Approximate Personalized Propagation of Neural Predictions (APPNP) method [23], which propagates the predictions obtained by a neural network on the node features to K steps away in a personalized PageRank-like scheme with a restart probability of α to generate final predictions. But the KProp is directly applied on the node features instead of the predictions with a restart probability of $\alpha = 0$ to exclude self-loops.

3.4 Locally Private GNN

Putting all together, the pseudo-code of the proposed privacy-preserving GNN training algorithm is presented in Algorithm 3, which will be ϵ -LDP according to the following corollary. Therefore, we call our method *Locally Private GNN (LPGNN)* algorithm.

COROLLARY 3.7. *Algorithm 3 satisfies ϵ -local differential privacy for graph nodes.*

Corollary 3.7 entails that the entire training procedure is ϵ -LDP due to the robustness of differential privacy to post-processing [10]. Furthermore, any prediction performed by the LPGNN is again subject to the post-processing theorem [10], and therefore, satisfies ϵ -LDP for the nodes, as the LDP mechanism is applied to the private data only once. Therefore, there is no need to add noise to the gradients of the model or use a perturbed objective function during training, even if the server decides to release the trained model.

4 EXPERIMENTS

We conduct extensive experiments to assess the privacy-utility performance of the proposed method for the node classification task and evaluate it under different parameter settings that can affect its effectiveness by answering the following research questions:

- **RQ1:** How does the performance of LPGNN compare to a standard GNN having zero privacy and a GNN which does not use node features having absolute (100%) privacy?

- **RQ2:** How accurate is the proposed multi-bit mechanism in estimating the neighborhood aggregation compared to other commonly used mechanisms?
- **RQ3:** How effective is the KProp neighborhood expansion method in increasing the accuracy of LPGNN?
- **RQ4:** How does the number of training nodes, known as the label rate, affect the performance of LPGNN?

4.1 Experimental settings

Datasets. In order to test the performance of the proposed method, we used two different sets of publicly available real-world datasets: three citation network datasets and three social network ones, as follows, whose statistics are summarized in Table 1:

- *Cora, Citeseer, and Pubmed* [45]: We used these well-known citation network datasets from, where each node represent a document, and edges denote citation links. Each node has a bag-of-words feature vector and a label indicating its category.
- *Facebook* [34]: This dataset is a page-page graph of verified Facebook sites. Nodes are official Facebook pages, and edges correspond to mutual likes between sites. Node features are extracted from the site descriptions, and the labels denote site category.
- *Github* [34]: This is a social network between Github developers, where nodes are users that have starred at least 10 repositories, and edges indicate mutual follower relationships. Node features are location, starred repositories, employer, and e-mail address. Nodes are labeled as being web or machine learning developer.
- *LastFM* [35]: This social network is collected from the music streaming service LastFM. Nodes denote users from Asian countries and links correspond to friendships. The task is to predict the home country of a user given the artists liked by them.

Comparative methods. We compare the performance of the proposed LPGNN method against the following ones:

- *GCN+RAW*: To see how our privacy-preserving method performs compared to the non-private case, we use a standard two-layer Graph Convolutional Network (GCN) [21] trained on the original features without any LDP perturbation, whose result can be considered as an upper-bound on the privacy-preserving methods.
- *GCN+RND*: As opposed to the previous method which has zero privacy protection, this method provides absolute privacy by training the previous GCN with randomly initialized node features (with the same dimension as the original features), which has been shown to perform reasonably well [3].
- *GCN+OHD*: This is another baseline with absolute privacy that uses one-hot encoding of node degrees, as in [43], instead of the original node features. To have a fair comparison, we also set the encoding dimension of this method equal to the previous ones’.

Experiment setup. For all the datasets, we randomly split nodes into training, validation, and test sets with 50/25/25% ratios, respectively. Without loss of generality, we normalized the node features of all the datasets between zero and one, so in all cases, we have $\alpha = 0$ and $\beta = 1$. We also generate random node features uniformly between zero and one for the GCN+RND method. For all the methods, we used a two-layer GCN having a hidden dimension of size 16 and the SeLU activation function [22] with batch normalization applied on the output of the first layer, but in LPGNN, the first GCN

Table 1: Descriptive statistics of the used datasets

DATASET	#CLASSES	#NODES	#EDGES	#FEATURES	AVG. DEG.
CORA	7	2,708	5,278	1,433	3.90
CITSEER	6	3,327	4,552	3,703	2.74
PUBMED	3	19,717	44,324	500	4.50
FACEBOOK	4	22,470	170,912	4,714	15.21
GITHUB	2	37,700	289,003	4,005	15.33
LASTFM	18	7,624	27,806	7,842	7.29

Table 2: Best found hyper-parameters used for experiments.

DATASET	LEARNING RATE	WEIGHT DECAY	DROPOUT
CORA	0.01	0.01	0
CITSEER	0.01	0.01	0
PUBMED	0.01	0.001	0
FACEBOOK	0.01	0.001	0.5
GITHUB	0.01	0	0.5
LASTFM	0.01	0.001	0.75

convolution layer is replaced by a KProp layer with the same hidden size and the same GCN aggregator function. We performed a combination of random and grid search in order to find the best choices for initial learning rate, weight decay, and dropout rate based on the validation performance of the GCN+RAW method, and used the same values for the other models. More specifically, we tried learning rate and weight decay both from $\{10^{-4}, 10^{-3}, 10^{-2}, 10^{-1}\}$, and dropout rate from $\{0, 0.25, 0.5, 0.75\}$. Table 2 displays the best performing hyper-parameters used for our experiments. All the models are trained using the cross-entropy loss function for node classification with the Adam optimizer [20] over a maximum of 500 epochs, and the best model is picked for testing based on the validation loss. We measured the Micro-F1 score on the test set over 10 consecutive runs and report the average and standard deviation of the results.

Hardware and software. The experiments were run on a remote server with Intel Xeon 6238 CPU and 60GB of available RAM, which was part of a Sun Grid Engine infrastructure. All the models were trained using a single NVIDIA V100 GPU having 32GB of graphic memory. The code were written in PyTorch 1.6.0 using PyTorch Geometric [12] version 1.6.1. Our implementation to reproduce the experimental results is publicly available at <https://github.com/sisaman/lpgnn>.

4.2 Experimental results

RQ1: analyzing the utility-privacy trade-off. We first evaluate how our privacy-preserving LPGNN method performs against the non-private and fully-private baselines in the node classification task under the varying privacy budget ϵ selected from $\{0.1, 0.5, 1, 2\}$. For each case, we searched for the best step parameter K of the LPGNN’s KProp layer from $\{1, 2, \dots, 32\}$ and picked the one with the best performance. Table 3 reports the micro averaged F1 score of different methods under different privacy budgets.

First of all, we observe that our LPGNN outperforms the fully-private methods in all cases, with an improvement ranging from around 2.5% on Github to over 19% on Pubmed. This result shows

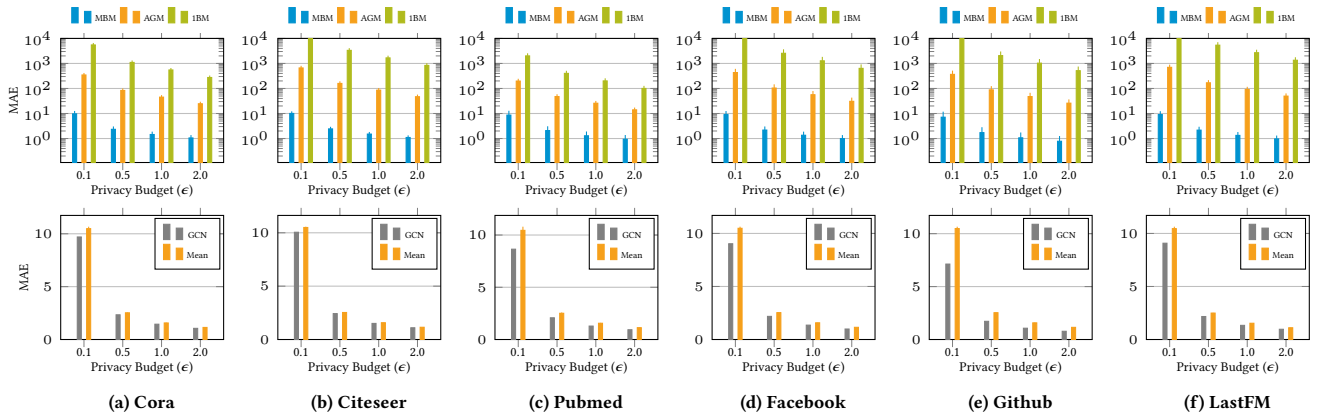


Figure 1: Performance of the multi-bit mechanism in estimating the neighborhood aggregation under different privacy budgets. The top row compares the mean absolute error (MAE) of the multi-bit (MBM), 1-bit (1BM), and the Analytic Gaussian (AGM) mechanisms. The bottom row compares the MAE of MBM obtained by the mean aggregator function against GCN’s.

that in addition to the graph structure, the node features in all the datasets are effective as well and their utility cannot be ignored.

Secondly, we can see that the LPGNN’s performance is comparable to the results obtained by the non-private GCN+RAW method, especially on the three social network datasets. The reason is that the initial average degree in these datasets is higher (see Table 1), which helps the aggregator function to drive out most of the noise in node features. Despite its low average degree, the performance of LPGNN across the Cora dataset is also very satisfactory with less than 1% accuracy loss, which is mainly due to the effectiveness of the KProp layer. On Citeseer and Pubmed, the accuracy loss is around 4 to 6% in the worst case, which is still acceptable for a privacy-preserving method.

Finally and most importantly, the performance of LPGNN stabilizes as the privacy budget (ϵ) decreases, showing almost no variations to the changes in ϵ , which demonstrates its robustness to higher noise injected by the LDP mechanism with lower privacy budgets. This is a promising property of LPGNN, because it allows using smaller values of ϵ for better privacy protection without sacrificing much of its accuracy.

RQ2: studying the multi-bit mechanism. In this experiment, we set to empirically evaluate the estimation accuracy of our multi-bit mechanism and compare it with the 1-bit mechanism [7], which is obtained by setting $m = d$ in Algorithm 1, and also the commonly used Gaussian mechanism [10], which adds a zero-mean Gaussian noise (whose variance depends on ϵ) to the data and is used for both single value and multidimensional data perturbation. Note that the Gaussian mechanism satisfies a relaxed version of ϵ -LDP, namely (ϵ, δ) -LDP, which (loosely speaking) means that it satisfies ϵ -LDP with probability at least $1 - \delta$. Here, we use the Analytic Gaussian mechanism [5], the optimized version of the standard Gaussian mechanism, with $\delta = 0.0001$ to make it close to our standard definition of ϵ -LDP. To compare the estimation performance of different mechanisms, we measure the mean absolute error (MAE) in the estimation of the neighborhood aggregator

Table 3: Micro-F1 score of different methods for node classification under varying privacy budget (ϵ).

DATASET	GCN +RAW	LPGNN				GCN +RND	GCN +OHD
		$\epsilon=0.1$	$\epsilon=0.5$	$\epsilon=1.0$	$\epsilon=2.0$		
CORA	85.2 ± 0.5	84.5 ± 0.6	84.5 ± 0.4	84.5 ± 0.5	84.8 ± 0.5	77.6 ± 1.0	57.7 ± 0.7
CITSEER	73.7 ± 0.5	68.3 ± 0.6	68.2 ± 0.9	68.1 ± 0.5	68.1 ± 0.8	52.8 ± 8.9	37.6 ± 0.9
PUBMED	86.8 ± 0.3	82.7 ± 0.2	82.5 ± 0.2	82.3 ± 0.2	82.3 ± 0.2	56.3 ± 1.8	63.0 ± 0.9
FACEBOOK	94.9 ± 0.1	93.9 ± 0.1	93.9 ± 0.2	93.9 ± 0.2	93.9 ± 0.2	39.4 ± 3.8	77.4 ± 0.5
GITHUB	86.7 ± 0.1	86.1 ± 0.1	86.1 ± 0.1	86.1 ± 0.2	86.0 ± 0.1	74.3 ± 0.0	83.7 ± 0.1
LASTFM	87.9 ± 0.3	86.0 ± 0.2	86.1 ± 0.3	86.0 ± 0.3	86.2 ± 0.3	21.4 ± 0.9	70.0 ± 0.5

defined by (5), calculated as:

$$MAE = \frac{1}{d|\mathcal{V}|} \sum_{v \in \mathcal{V}} \left\| \hat{h}_{\mathcal{N}(v)} - h_{\mathcal{N}(v)} \right\|_1 \quad (10)$$

where $\|\cdot\|_1$ is the L1-norm. First, we look at how the LDP mechanisms perform in terms of the estimation error with respect to different values of the privacy budget ϵ . To this end, we vary the value of ϵ within $\{0.1, 0.5, 1, 2\}$, and calculate the MAE of all the mechanisms, illustrated in Figure 1 (top row). We see that in all cases, our multi-bit method produces a considerably lower error compared to both the Analytic Gaussian and the 1-bit mechanism, consistently over all the datasets. This is because the variance of the optimized multi-bit mechanism is lower than that of the 1-bit mechanism (as shown in Proposition 3.5) and the Gaussian mechanism, resulting in a more accurate estimation. At the same time, our mechanism is also efficient in terms of the communication overhead, requiring only two bits per feature, while the Gaussian mechanism’s output is real-valued, usually taking 32 bits per

feature (more or less, depending on the precision) to transmit a floating-point number.

We also evaluated the effect of the aggregator function on the estimation error of the multi-bit mechanism. For this purpose, we measured the MAE of the multi-bit mechanism with two commonly used linear aggregator functions: (i) the mean aggregator: $h_{\mathcal{N}(v)} = \frac{1}{|\mathcal{N}(v)|} \sum_{u \in \mathcal{N}(v)} x_u$; and (ii) the GCN aggregator: $h_{\mathcal{N}(v)} = \frac{\sum_{u \in \mathcal{N}(v)} x_u}{\sqrt{|\mathcal{N}(u)| \cdot |\mathcal{N}(v)|}}$, under different values of $\epsilon \in \{0.1, 0.5, 1, 2\}$. According to the results depicted in Figure 1 (bottom row), using the GCN aggregator leads to a lower estimation error in all cases. This is due to the difference in the normalization factor used in these aggregator functions that affect their estimation variance. More specifically, the normalization factor in the GCN aggregator is $\sqrt{|\mathcal{N}(u)| \cdot |\mathcal{N}(v)|}$, while for the mean, it is $|\mathcal{N}(u)| = \sqrt{|\mathcal{N}(v)| \cdot |\mathcal{N}(v)|}$. In other words, the GCN aggregator considers the square root of the degree of both the central node v and its neighbor u , whereas the mean aggregator considers the square root of the degree of only the central node v twice. As in many real graphs there are much more of low degree nodes than high degree ones, when using the mean aggregator the normalization factor is small for most of the nodes, leading to a high estimation variance. But as many of the low degree nodes are linked to high degree ones, the GCN aggregator tends to balance the normalization by considering the degree of both link endpoints. Consequently, the normalization for many low degree nodes increases compared to the mean aggregator, yielding a lower estimation variance.

RQ3: studying the effect of KProp. In this experiment, we investigate whether the KProp layer is effective in gaining performance boost. For this purpose, we varied the KProp’s step parameter (K) from $\{1, 2, \dots, 32\}$, and trained the LPGNN model under different privacy budgets (ϵ) selected from $\{0.01, 0.1, 1.0\}$. We also evaluate the effect of the KProp when using the original private data by replacing the first layer of the GCN+RAW with a KProp. Figure 2 (top row) illustrates the results. First of all, we see that using KProp with standard GCN in the non-private setting hurts the performance of the classifier with increasing K . This is because repeatedly aggregating features from far nodes over-smooths the aggregation [28], leading to performance loss. However, the story is quite different when dealing with noisy, differentially private data, as it is evident in the figure. We can observe that under all the privacy budgets tried, the performance of the LPGNN rises up to an extent by increasing K , which shows that the model can benefit from larger population sizes to have a better estimation of the neighborhood aggregation. We see that the amount of the privacy budget does not have a tangible impact on the result, which again proves the robustness of the method to higher amounts of noise. On the other hand, according to the results, the maximum performance gain depends on the average node degree of the dataset. For instance, over the social network datasets with a higher average degree, the accuracy improvement goes from over 2% on Facebook at $K = 8$ to about 5% on Github at $K = 16$ relative to the case of $K = 1$, while over lower-degree citation networks, it ranges from near 5% on Citeseer to around 8% on Pubmed both at $K = 32$. The maximum step parameter K that yields the best result does also depend on the average degree of the graph. For example, we see that

the trend is still increasing even at $K = 32$ over citation networks with a lower average degree, whereas the accuracy begins to fall down over higher-degree social networks after $K = 8$.

Figure 2 (bottom row) also analyzes the effect of adding or removing self-loops on the classification performance when using the KProp layer with K varying from 1 to 32 and ϵ fixed to 1. We can see from the figure that the results obtained while removing self-loops are usually superior to the case of adding self-loops, especially with smaller K s, and the highest accuracy is achieved with self-loops removed. As mentioned in Section 3, this is because adding self-loops causes the KProp to count the same nodes multiple times in the final aggregation, which accumulates the repetitive noise and thus degrades the estimation accuracy.

RQ4: analyzing the effect of label rate. In this final experiment, we investigate how does the label rate, which is the fraction of labeled nodes used for training to the total number of nodes in the graph, affect the performance of LPGNN under different privacy budgets and KProp step parameters. Since all the datasets were split using 50/25/25% ratios, maximum 50% of the nodes are used for training in the previous experiments. Here, we vary the label rate ρ from $\{10\%, 20\%, \dots, 50\%\}$ and train LPGNN only with ρ fraction of nodes as the training data.

First, we fix the KProp step $K = 4$ and change the privacy budget ϵ from $\{0.01, 0.1, 1\}$, whose result is exhibited in Figure 3 (top row). As we see, increasing the label rate elevates the accuracy of LPGNN in all cases. This is mainly due to the node features being noisy, so with fewer training nodes, the model overfits to the noise injected by LDP and thus loses its ability to generalize well over unseen test data. But with more training nodes, the model eventually learns how to deal with the noise. Furthermore, as the label rate grows, we notice that the difference between the results obtained under different privacy budgets gradually decreases and tends to converge to zero (which we witnessed in Table 3). This again is a promising result that enables us to deliver better privacy protections by lowering the privacy budget and then compensate the noise by providing more of the training data.

Finally, we fix $\epsilon = 1$ and vary the KProp step parameter K in $\{1, 2, 4\}$ to check how the label rate and KProp jointly affect LPGNN’s performance. The result is depicted in Figure 3 (bottom row). We observe that the effect of KProp is more evident when the label rate is low. For instance, with a 10% label rate, KProp with $K = 4$ yielded an accuracy boost of about 7%, 10%, and 15%, on Pubmed, Cora, and LastFM, respectively. This is because with lower label rates, due to the lack of enough training data, the model cannot learn to handle the noise on its own, and therefore KProp can better serve the model by canceling out most of the noise in the neighborhood aggregation. Although KProp can be still useful with higher label rates (as we witnessed before), the abundance of training nodes also helps the model learn to mitigate the noise.

5 DISCUSSION

Not all kinds of deep learning models are robust to differentially private input data, as the noise will usually go through multiple layers of non-linearity, which significantly affects their utility [50]. However, we systematically showed that this is not the case for GNNs, as in these models the noise added to the data will average out in

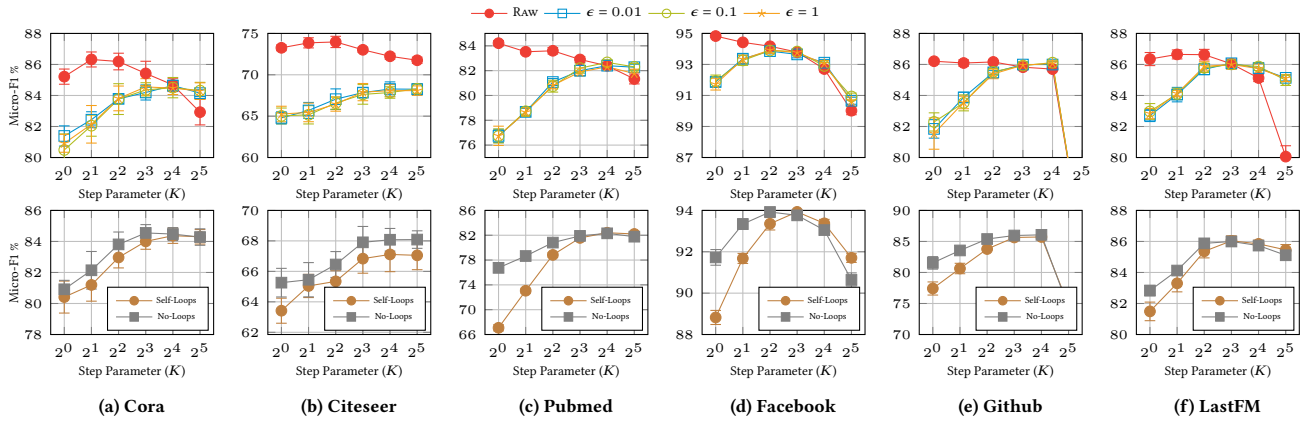


Figure 2: Effect of the KProp step parameter (K) on the performance of LPGNN. The top row compares the node classification’s Micro-F1 score under LDP perturbation with different values of ϵ , as well as using raw features (without perturbation). The bottom row illustrates the effect of removing self-loops at $\epsilon = 1$. Note that the y-axis is not set to zero to focus on the trends.

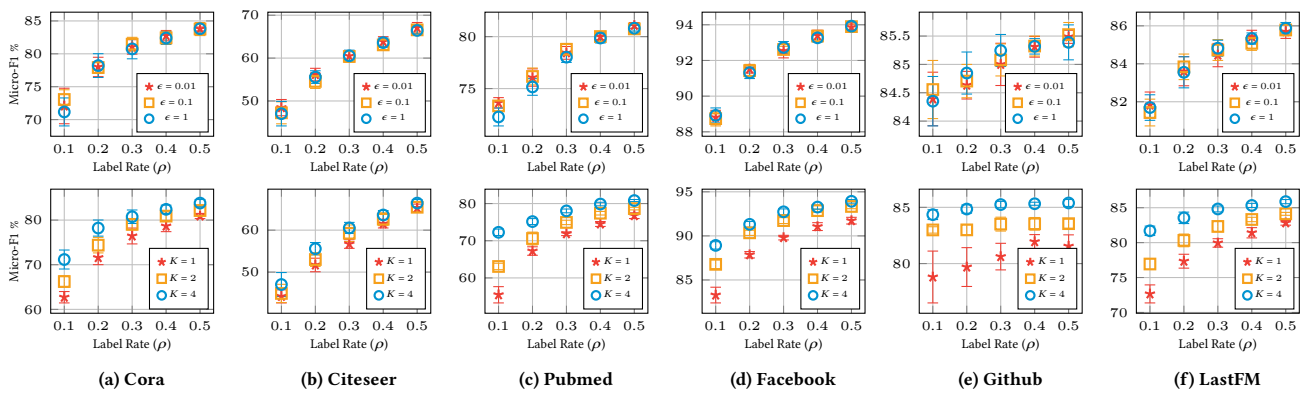


Figure 3: Effect of the label rate (ρ) on the performance of LPGNN. Top: results for varying privacy budgets (ϵ) with fixed $K = 8$. Bottom: results for varying KProp step parameters (K) with $\epsilon = 1.0$ fixed. Note that the y-axis is not set to zero.

the neighborhood aggregation step before applying the non-linear transformation, making them robust to differentially private input data. As a result, GNN-based deep learning models can be used not only to solve the introduced node-level privacy problem, but also as an alternative solution to other privacy-preserving approaches to address more general supervised learning tasks in which the training data cannot leave users’ devices due to privacy constraints.

Our proposed framework has three privacy-related hyperparameters, α , β , and ϵ , which are sent to the nodes by the server. The proposed framework requires that the server knows the range of private features, which is a common assumption in the literature [8]. Technically, the server can either guess the range of the features (e.g. between 00:00 and 23:59 if it represents time) or could use other privacy-preserving methods, such as secure multi-party computation [37], as a pre-processing step to determine range parameters.

Note that if, for any node, the requested feature lied outside the provided range (e.g. due to inaccurate guessing), the node can simply clip its feature within the given bound.

Probably, the most important parameter of our method is the privacy budget ϵ , which controls the trade-off between the accuracy of the GNN and the strength of the privacy guarantee. While there are some efforts trying to systematically determine ϵ in differentially private applications [16, 26], still there is no general guideline for choosing the best value for ϵ , since the privacy guarantees enforced by differential privacy are very different based on the data domain and the target query. Therefore, previous works [7, 38] usually evaluate their systems by trying different values of ϵ , and then pick the smallest one resulting in an acceptable performance for the deployment. For instance, Microsoft uses $\epsilon = 1$ to collect telemetry data from Windows users [7], while Apple’s choice of ϵ in iOS and macOS ranges between 2 and 8 [38]. In our experiments, however,

we have seen that our model is completely robust even to small ϵ values less than 1.

6 RELATED WORK

Recent years have seen a surge in applying GNNs for representation learning over graphs, and numerous GNN models have been proposed for graph representation learning, including Graph Convolutional Networks (GCN) [21], Graph Attention Networks (GAT) [39], GraphSAGE [13], Graph Isomorphism Networks (GIN) [43], and so on. We refer the reader to the available surveys on GNNs [14, 41] for other models and discussion on their performance and applications.

To address the privacy issue when the data is sensitive and cannot be released to untrusted third-parties for model training, numerous techniques have been proposed, which are mostly based on homomorphic encryption [15], secure multiparty computation [33], and federated learning [25]. Differential privacy has also been successfully adapted to preserve training data privacy [1, 48]. However, these approaches are mostly designed for training conventional deep neural networks over structured data, such as images or text.

While there is a growing interest in both theory and applications of GNNs, there have been only a few attempts to provide privacy-preserving graph representation learning algorithms. Xu *et al.* [42] proposed a differentially private graph embedding method by applying the objective perturbation on the loss function of matrix factorization. Zhang and Ni [47] proposed a differentially private perturbed gradient descent method based on Lipschitz condition [17] for matrix factorization-based graph embedding. But both of these methods target classic graph embedding algorithms and not GNNs. Li *et al.* [27] presented a graph adversarial training framework that integrates disentangling and purging mechanisms to remove users' private information from learned node representations. But unlike our paper, they assume that the server who trains the model has complete access to the private data.

There are also recent approaches that attempted to address privacy in GNNs using federated and split learning. Mei *et al.* [29] proposed a similarity-based GNN based on structural similarity and federated learning to hide content and structure information. Zhou *et al.* [49] tackled the problem of privacy-preserving node classification by splitting the computation graph of a GNN between multiple data holders, and use a trusted server to combine the information from different parties and complete the training. However, as opposed to our method, these approaches rely on the existence of a trusted third party for model aggregation, and also their privacy protection is not formally guaranteed. Finally, Jiang *et al.* [18] proposed a distributed and secure framework to learn the object representations in video data from graph sequences based on GNN and federated learning, and design secure aggregation primitives to protect the privacy in federated learning. However, they assume that each party owns a series of graphs (extracted from video data) and the server uses federated learning to learn an inductive GNN over this distributed dataset of graphs, which is a totally different problem setting than the node-level privacy we studied.

7 CONCLUSION

In this paper, we presented a locally differentially private GNN to address the problem of node-level privacy, when graph nodes

have sensitive attributes that are kept private, but they could be advantageous to a GNN for learning rich node representations by a central server. To this end, we first proposed the *multi-bit mechanism*, a multidimensional ϵ -LDP algorithm that allows the server to privately collect node features. We then presented an unbiased estimator for the server by which it can estimate the first-layer graph convolution of the GNN using the noisy features. Finally, to further decrease the estimation error, we introduced KProp, a simple graph convolution layer that aggregates features from higher-order neighbors. Experimental experiments over real-world graph datasets on the node classification task demonstrated that the proposed framework can maintain an appropriate privacy-utility trade-off in learning representation for graph nodes.

The concept of privacy-preserving graph representation learning is a novel and unexplored field of research with many potential future directions that can go beyond node-level privacy, such as link-level privacy and graph-level privacy. For the presented work, several potential future directions and improvements are imaginable. Firstly, we would like to explore other neighborhood expansion mechanisms that are more effective than the proposed KProp. Secondly, in this paper, we used the same number of features to be perturbed by the multi-bit mechanism for all the nodes, whose value was obtained by minimizing the worst-case variance of the multi-bit estimator. As future work, we set to investigate an optimized heterogeneous feature perturbation scheme by minimizing a variance-based loss function over the entire network. Finally, we intend to combine the proposed LPGNN with graph structure learning methods to address privacy-preserving classification over non-relational datasets with much less communication overhead compared to other approaches, such as federated learning.

ACKNOWLEDGMENTS

We would like to thank Emiliano De Cristofaro, Hamed Haddadi, Nikolaos Karaliyas, and Mohammad Malekzadeh for their helpful advice and comments on the paper. This work is supported as part of the Dusk2Dawn project by the Swiss National Science Foundation (SNSF) through the Sinergia interdisciplinary program under grant number 173696.

REFERENCES

- [1] M. Abadi, A. Chu, I. Goodfellow, H. Brendan McMahan, I. Mironov, K. Talwar, and L. Zhang. 2016. Deep Learning with Differential Privacy. *ArXiv e-prints* (July 2016). arXiv:1607.00133 [stat.ML]
- [2] Mart í n Abadi, Andy Chu, Ian Goodfellow, H Brendan McMahan, Ilya Mironov, Kunal Talwar, and Li Zhang. 2016. Deep learning with differential privacy. In *Proceedings of the 2016 ACM SIGSAC Conference on Computer and Communications Security*. ACM, 308–318.
- [3] Ralph Abboud, İsmail İlkan Ceylan, Martin Grohe, and Thomas Lukasiewicz. 2020. The Surprising Power of Graph Neural Networks with Random Node Initialization. *arXiv preprint arXiv:2010.01179* (2020).
- [4] Sami Abu-El-Hajja, Bryan Perozzi, Amol Kapoor, Nazanin Alipourfard, Kristina Lerman, Hrayr Harutyunyan, Greg Ver Steeg, and Aram Galstyan. 2019. Mix H op: Higher-Order Graph Convolutional Architectures via Sparsified Neighborhood Mixing (*Proceedings of Machine Learning Research, Vol. 97*), Kamalika Chaudhuri and Ruslan Salakhutdinov (Eds.). PMLR, Long Beach, California, USA, 21–29.
- [5] Borja Balle and Yu-Xiang Wang. 2018. Improving the Gaussian Mechanism for Differential Privacy: Analytical Calibration and Optimal Denoising. In *International Conference on Machine Learning*. 394–403.
- [6] Zhengdao Chen, Xiang Li, and Joan Bruna. 2017. Supervised community detection with line graph neural networks. *arXiv preprint arXiv:1705.08415* (2017).
- [7] Bolin Ding, Janardhan Kulkarni, and Sergey Yekhanin. 2017. Collecting telemetry data privately. In *Advances in Neural Information Processing Systems*. 3571–3580.

- [8] John C Duchi, Michael I Jordan, and Martin J Wainwright. 2018. Minimax optimal procedures for locally private estimation. *J. Amer. Statist. Assoc.* 113, 521 (2018), 182–201.
- [9] David K Duvenaud, Dougal Maclaurin, Jorge Iparraguirre, Rafael Bombarell, Timothy Hirzel, Alán Aspuru-Guzik, and Ryan P Adams. 2015. Convolutional networks on graphs for learning molecular fingerprints. In *Advances in neural information processing systems*. 2224–2232.
- [10] Cynthia Dwork, Aaron Roth, et al. 2014. The algorithmic foundations of differential privacy. *Foundations and Trends® in Theoretical Computer Science* 9, 3–4 (2014), 211–407.
- [11] Wenqi Fan, Yao Ma, Qing Li, Yuan He, Eric Zhao, Jiliang Tang, and Dawei Yin. 2019. Graph neural networks for social recommendation. In *The World Wide Web Conference*. 417–426.
- [12] Matthias Fey and Jan E. Lenssen. 2019. Fast Graph Representation Learning with PyTorch Geometric. In *ICLR Workshop on Representation Learning on Graphs and Manifolds*.
- [13] Will Hamilton, Zhitao Ying, and Jure Leskovec. 2017. Inductive representation learning on large graphs. In *Advances in neural information processing systems*. 1024–1034.
- [14] William L Hamilton, Rex Ying, and Jure Leskovec. 2017. Representation learning on graphs: Methods and applications. *arXiv preprint arXiv:1709.05584* (2017).
- [15] Ehsan Hesamifard, Hassan Takabi, Mehdi Ghasemi, and Rebecca N Wright. 2018. Privacy-preserving machine learning as a service. *Proceedings on Privacy Enhancing Technologies* 2018, 3 (2018), 123–142.
- [16] Justin Hsu, Marco Gaboardi, Andreas Haeberlen, Sanjeev Khanna, Arjun Narayan, Benjamin C Pierce, and Aaron Roth. 2014. Differential privacy: An economic method for choosing epsilon. In *2014 IEEE 27th Computer Security Foundations Symposium*. IEEE, 398–410.
- [17] Madhav Jha and Sofya Raskhodnikova. 2013. Testing and reconstruction of Lipschitz functions with applications to data privacy. *SIAM J. Comput.* 42, 2 (2013), 700–731.
- [18] Meng Jiang, Taeho Jung, Ryan Karl, and Tong Zhao. 2020. Federated Dynamic GNN with Secure Aggregation. *arXiv preprint arXiv:2009.07351* (2020).
- [19] Shiva Prasad Kasiviswanathan, Homin K Lee, Kobbi Nissim, Sofya Raskhodnikova, and Adam Smith. 2011. What can we learn privately? *SIAM J. Comput.* 40, 3 (2011), 793–826.
- [20] Diederik P Kingma and Jimmy Ba. 2014. Adam: A method for stochastic optimization. *arXiv preprint arXiv:1412.6980* (2014).
- [21] Thomas N. Kipf and Max Welling. 2017. Semi-Supervised Classification with Graph Convolutional Networks. In *International Conference on Learning Representations (ICLR)*.
- [22] Günter Klambauer, Thomas Unterthiner, Andreas Mayr, and Sepp Hochreiter. 2017. Self-normalizing neural networks. In *Advances in neural information processing systems*. 971–980.
- [23] Johannes Klicpera, Aleksandar Bojchevski, and Stephan Günnemann. 2019. Predict then Propagate: Graph Neural Networks meet Personalized PageRank. In *International Conference on Learning Representations (ICLR)*.
- [24] Johannes Klicpera, Stefan Weißenberger, and Stephan Günnemann. 2019. Diffusion improves graph learning. In *Advances in Neural Information Processing Systems*. 13354–13366.
- [25] Jakub Konečný, H. Brendan McMahan, Felix X. Yu, Peter Richtarik, Ananda Theertha Suresh, and Dave Bacon. 2016. Federated Learning: Strategies for Improving Communication Efficiency. In *NIPS Workshop on Private Multi-Party Machine Learning*.
- [26] Jaewoo Lee and Chris Clifton. 2011. How Much Is Enough? Choosing ϵ for Differential Privacy. In *Information Security*, Xuejia Lai, Jianying Zhou, and Hui Li (Eds.). Springer Berlin Heidelberg, Berlin, Heidelberg, 325–340.
- [27] Kaiyang Li, Guangchun Luo, Yang Ye, Wei Li, Shihao Ji, and Zhipeng Cai. 2020. Adversarial Privacy Preserving Graph Embedding against Inference Attack. *arXiv preprint arXiv:2008.13072* (2020).
- [28] Qimai Li, Zhichao Han, and Xiao-Ming Wu. 2018. Deeper insights into graph convolutional networks for semi-supervised learning. *arXiv preprint arXiv:1801.07606* (2018).
- [29] G. Mei, Z. Guo, S. Liu, and L. Pan. 2019. SGNN: A Graph Neural Network Based Federated Learning Approach by Hiding Structure. In *2019 IEEE International Conference on Big Data (Big Data)*. IEEE Computer Society, Los Alamitos, CA, USA, 2560–2568.
- [30] Christopher Morris, Martin Ritzert, Matthias Fey, William L Hamilton, Jan Eric Lenssen, Gaurav Rattan, and Martin Grohe. 2019. Weisfeiler and leman go neural: Higher-order graph neural networks. In *Proceedings of the AAAI Conference on Artificial Intelligence*, Vol. 33. 4602–4609.
- [31] AJ Paverd, Andrew Martin, and Ian Brown. 2014. Modelling and automatically analysing privacy properties for honest-but-curious adversaries. *Tech. Rep.* (2014).
- [32] Sungmin Rhee, Seokjun Seo, and Sun Kim. 2017. Hybrid approach of relation network and localized graph convolutional filtering for breast cancer subtype classification. *arXiv preprint arXiv:1711.05859* (2017).
- [33] Bitan Darvish Rouhani, M Sadegh Riazi, and Farinaz Koushanfar. 2017. DeepSecure: Scalable Provably-Secure Deep Learning. *arXiv preprint arXiv:1705.08963* (2017).
- [34] Benedek Rozemberczki, Carl Allen, and Rik Sarkar. 2019. Multi-scale Attributed Node Embedding. *arXiv preprint arXiv:1909.13021* (2019).
- [35] Benedek Rozemberczki and Rik Sarkar. 2020. Characteristic Functions on Graphs: Birds of a Feather, from Statistical Descriptors to Parametric Models. In *Proceedings of the 29th ACM International Conference on Information and Knowledge Management (CIKM '20)*. ACM.
- [36] Franco Scarselli, Marco Gori, Ah Chung Tsoi, Markus Hagenbuchner, and Gabriele Monfardini. 2008. The graph neural network model. *IEEE Transactions on Neural Networks* 20, 1 (2008), 61–80.
- [37] R. Sheikh and D. K. Mishra. 2010. Protocols for Getting Maximum Value for Multi-Party Computations. In *2010 Fourth Asia International Conference on Mathematical/Analytical Modelling and Computer Simulation*. 597–600.
- [38] Jun Tang, Aleksandra Korolova, Xiaolong Bai, Xueqiang Wang, and Xiaofeng Wang. 2017. Privacy loss in apple’s implementation of differential privacy on macos 10.12. *arXiv preprint arXiv:1709.02753* (2017).
- [39] Petar Veličković, Guillem Cucurull, Arantxa Casanova, Adriana Romero, Pietro Lio, and Yoshua Bengio. 2017. Graph attention networks. *arXiv preprint arXiv:1710.10903* (2017).
- [40] Felix Wu, Amauri Souza, Tianyi Zhang, Christopher Fifty, Tao Yu, and Kilian Weinberger. 2019. Simplifying Graph Convolutional Networks (*Proceedings of Machine Learning Research, Vol. 97*). Kamalika Chaudhuri and Ruslan Salakhutdinov (Eds.). PMLR, Long Beach, California, USA, 6861–6871.
- [41] Zonghan Wu, Shirui Pan, Fengwen Chen, Guodong Long, Chengqi Zhang, and S Yu Philip. 2020. A comprehensive survey on graph neural networks. *IEEE Transactions on Neural Networks and Learning Systems* (2020).
- [42] Depeng Xu, Shuhan Yuan, Xintao Wu, and HaiNhat Phan. 2018. DPNE: Differentially private network embedding. In *Pacific-Asia Conference on Knowledge Discovery and Data Mining*. Springer, 235–246.
- [43] Keyulu Xu, Weihua Hu, Jure Leskovec, and Stefanie Jegelka. 2018. How powerful are graph neural networks? *arXiv preprint arXiv:1810.00826* (2018).
- [44] Mengmeng Yang, Lingjuan Lyu, Jun Zhao, Tianqing Zhu, and Kwok-Yan Lam. 2020. Local Differential Privacy and Its Applications: A Comprehensive Survey. *arXiv preprint arXiv:2008.03686* (2020).
- [45] Zhilin Yang, William W Cohen, and Ruslan Salakhutdinov. 2016. Revisiting semi-supervised learning with graph embeddings. *arXiv preprint arXiv:1603.08861* (2016).
- [46] Muhan Zhang and Yixin Chen. 2018. Link prediction based on graph neural networks. In *Advances in Neural Information Processing Systems*. 5165–5175.
- [47] Sen Zhang and Weiwei Ni. 2019. Graph Embedding Matrix Sharing With Differential Privacy. *IEEE Access* 7 (2019), 89390–89399.
- [48] Lingchen Zhao, Qian Wang, Qin Zou, Yan Zhang, and Yanjiao Chen. 2019. Privacy-preserving collaborative deep learning with unreliable participants. *IEEE Transactions on Information Forensics and Security* 15 (2019), 1486–1500.
- [49] Jun Zhou, Chaochao Chen, Longfei Zheng, Xiaolin Zheng, Bingzhe Wu, Ziqi Liu, and Li Wang. 2020. Privacy-Preserving Graph Neural Network for Node Classification. *arXiv preprint arXiv:2005.11903* (2020).
- [50] T. Zhu, D. Ye, W. Wang, W. Zhou, and P. Yu. 2020. More Than Privacy: Applying Differential Privacy in Key Areas of Artificial Intelligence. *IEEE Transactions on Knowledge & Data Engineering* 1, 01 (aug 2020), 1–1.

A DEFERRED THEORETICAL ARGUMENTS

A.1 Theorem 3.1

PROOF. Let $\mathcal{M}(x)$ denote the multi-bit mechanism (Algorithm 1) applied on the input vector x . Let $x^* = \mathcal{M}(x)$ be the perturbed vector corresponding to x . We need to show that for any two input features x_1 and x_2 , we have $\frac{\Pr[\mathcal{M}(x_1)=x^*]}{\Pr[\mathcal{M}(x_2)=x^*]} \leq e^\epsilon$.

According to Algorithm 1, for any dimension $i \in \{1, 2, \dots, d\}$, it can be easily seen that $x_i^* \in \{-1, 0, 1\}$. The case $x_i^* = 0$ occurs when $i \notin S$ with probability $1 - \frac{m}{d}$, therefore:

$$\frac{\Pr[\mathcal{M}(x_1)_i = 0]}{\Pr[\mathcal{M}(x_2)_i = 0]} = \frac{1 - m/d}{1 - m/d} = 1 \leq e^\epsilon, \quad \forall \epsilon > 0 \quad (11)$$

For $x_i^* \in \{-1, 1\}$ and according to Algorithm 1, we see that the probability of getting $x_i^* = 1$ ranges from $\frac{m}{d} \cdot \frac{1}{e^{\epsilon/m+1}}$ to $\frac{m}{d} \cdot \frac{e^{\epsilon/m}}{e^{\epsilon/m+1}}$ depending on the value of x_i . Analogously, the probability of $x_i^* =$

-1 also varies from $\frac{m}{d} \cdot \frac{1}{e^{\epsilon/m+1}}$ to $\frac{m}{d} \cdot \frac{e^{\epsilon/m}}{e^{\epsilon/m+1}}$. Therefore:

$$\begin{aligned} \frac{\Pr[\mathcal{M}(x_1)_i \in \{-1, 1\}]}{\Pr[\mathcal{M}(x_2)_i \in \{-1, 1\}]} &\leq \frac{\max \Pr[\mathcal{M}(x_1)_i \in \{-1, 1\}]}{\min \Pr[\mathcal{M}(x_2)_i \in \{-1, 1\}]} \\ &\leq \frac{\frac{m}{d} \cdot \frac{e^{\epsilon/m}}{e^{\epsilon/m+1}}}{\frac{m}{d} \cdot \frac{1}{e^{\epsilon/m+1}}} \leq e^{\epsilon/m} \end{aligned} \quad (12)$$

Consequently, we have:

$$\begin{aligned} \frac{\Pr[\mathcal{M}(x_1) = x^*]}{\Pr[\mathcal{M}(x_2) = x^*]} &= \prod_{i=1}^d \frac{\Pr[\mathcal{M}(x_1)_i = x_i^*]}{\Pr[\mathcal{M}(x_2)_i = x_i^*]} \\ &= \prod_{j|x_j^*=0} \frac{\Pr[\mathcal{M}(x_1)_j = 0]}{\Pr[\mathcal{M}(x_2)_j = 0]} \\ &\quad \times \prod_{k|x_k^* \in \{-1, 1\}} \frac{\Pr[\mathcal{M}(x_1)_k \in \{-1, 1\}]}{\Pr[\mathcal{M}(x_2)_k \in \{-1, 1\}]} \end{aligned} \quad (13)$$

$$= \prod_{x_k^* \in \{-1, 1\}} \frac{\Pr[\mathcal{M}(x_1)_k \in \{-1, 1\}]}{\Pr[\mathcal{M}(x_2)_k \in \{-1, 1\}]} \quad (14)$$

$$\leq \prod_{x_k^* \in \{-1, 1\}} e^{\epsilon/m} \quad (15)$$

$$\leq e^{\epsilon} \quad (16)$$

which concludes the proof. In the above, (14) and (15) follows from applying (11) and (12), respectively, and (16) follows from the fact that exactly m number of input features result in non-zero output. \square

A.2 Proposition 3.2

We first establish the following lemma and then prove Proposition 3.2:

LEMMA A.1. *Let x^* be the output of Algorithm 1 on the input vector x . For any dimension $i \in \{1, 2, \dots, d\}$, we have:*

$$\mathbb{E}[x_i^*] = \frac{m}{d} \cdot \frac{e^{\epsilon/m} - 1}{e^{\epsilon/m+1}} \cdot \left(2 \cdot \frac{x_i - \alpha}{\beta - \alpha} - 1 \right) \quad (17)$$

and

$$\text{Var}[x_i^*] = \frac{m}{d} - \left[\frac{m}{d} \cdot \frac{e^{\epsilon/m} - 1}{e^{\epsilon/m+1}} \cdot \left(2 \cdot \frac{x_i - \alpha}{\beta - \alpha} - 1 \right) \right]^2 \quad (18)$$

PROOF. For the expectation, we have:

$$\begin{aligned} \mathbb{E}[x_i^*] &= \mathbb{E}[x_i^* | s_i = 0] \Pr(s_i = 0) + \mathbb{E}[x_i^* | s_i = 1] \Pr(s_i = 1) \\ &= \frac{m}{d} \cdot (2 \mathbb{E}[t_i] - 1) \end{aligned} \quad (19)$$

Since t_i is a Bernoulli random variable, we have:

$$\mathbb{E}[t_i] = \frac{1}{e^{\epsilon/m+1}} + \frac{x_i - \alpha}{\beta - \alpha} \cdot \frac{e^{\epsilon/m} - 1}{e^{\epsilon/m+1}} \quad (20)$$

Combining (19) and (20) yields:

$$\begin{aligned} \mathbb{E}[x_i^*] &= \frac{m}{d} \cdot \left[2 \left(\frac{1}{e^{\epsilon/m+1}} + \frac{x_i - \alpha}{\beta - \alpha} \cdot \frac{e^{\epsilon/m} - 1}{e^{\epsilon/m+1}} \right) - 1 \right] \\ &= \frac{m}{d} \cdot \left[\frac{1 - e^{\epsilon/m}}{e^{\epsilon/m+1}} + 2 \cdot \frac{x_i - \alpha}{\beta - \alpha} \cdot \frac{e^{\epsilon/m} - 1}{e^{\epsilon/m+1}} \right] \\ &= \frac{m}{d} \cdot \frac{e^{\epsilon/m} - 1}{e^{\epsilon/m+1}} \cdot \left(2 \cdot \frac{x_i - \alpha}{\beta - \alpha} - 1 \right) \end{aligned} \quad (21)$$

For the variance, we have:

$$\begin{aligned} \text{Var}[x_i^*] &= \mathbb{E}[(x_i^*)^2] - \mathbb{E}[x_i^*]^2 \\ &= \mathbb{E}[(x_i^*)^2 | s_i = 0] \Pr(s_i = 0) \\ &\quad + \mathbb{E}[(x_i^*)^2 | s_i = 1] \Pr(s_i = 1) - \mathbb{E}[x_i^*]^2 \end{aligned}$$

Given $s_i = 1$, we have $x_i^* = \pm 1$, and thus $(x_i^*)^2 = 1$. Therefore, combining with (21), we get:

$$\text{Var}[x_i^*] = \frac{m}{d} - \left[\frac{m}{d} \cdot \frac{e^{\epsilon/m} - 1}{e^{\epsilon/m+1}} \cdot \left(2 \cdot \frac{x_i - \alpha}{\beta - \alpha} - 1 \right) \right]^2 \quad (22)$$

\square

Now we prove Proposition 3.2.

PROOF. We need to show that $\mathbb{E}[x'_{v,i}] = x_{v,i}$ for any $v \in \mathcal{V}$ and any dimension $i \in \{1, 2, \dots, d\}$.

$$\mathbb{E}[x'_{v,i}] = \frac{d(\beta - \alpha)}{2m} \cdot \frac{e^{\epsilon/m} + 1}{e^{\epsilon/m} - 1} \cdot \mathbb{E}[x_{v,i}^*] + \frac{\alpha + \beta}{2} \quad (23)$$

Applying Lemma A.1 yields:

$$\begin{aligned} \mathbb{E}[x'_{v,i}] &= \frac{d(\beta - \alpha)}{2m} \cdot \frac{e^{\epsilon/m} + 1}{e^{\epsilon/m} - 1} \left[\frac{m}{d} \cdot \frac{e^{\epsilon/m} - 1}{e^{\epsilon/m+1}} \left(2 \cdot \frac{x_{v,i} - \alpha}{\beta - \alpha} - 1 \right) \right] \\ &\quad + \frac{\alpha + \beta}{2} \\ &= \frac{\beta - \alpha}{2} \left(2 \cdot \frac{x_{v,i} - \alpha}{\beta - \alpha} - 1 \right) + \frac{\alpha + \beta}{2} \\ &= x_{v,i} - \alpha - \frac{\beta - \alpha}{2} + \frac{\alpha + \beta}{2} = x_{v,i} \end{aligned}$$

\square

A.3 Corollary 3.3

PROOF. We need to show that the following holds for any node $v \in \mathcal{V}$:

$$\mathbb{E}[\widehat{h}_{\mathcal{N}(v)}] = h_{\mathcal{N}(v)}$$

The left hand side of the above can be written as:

$$\mathbb{E}[\widehat{h}_{\mathcal{N}(v)}] = \mathbb{E}[\text{AGGREGATE}(\{x'_u, \forall u \in \mathcal{N}(v)\})]$$

Since AGGREGATE is linear, due to the linearity of expectation, the expectation sign can be moved inside AGGREGATE:

$$\mathbb{E}[\widehat{h}_{\mathcal{N}(v)}] = \text{AGGREGATE}(\{\mathbb{E}[x'_u], \forall u \in \mathcal{N}(v)\})$$

Finally, by Proposition 3.2, we have:

$$\mathbb{E}[\widehat{h}_{\mathcal{N}(v)}] = \text{AGGREGATE}(\{x_u, \forall u \in \mathcal{N}(v)\}) = h_{\mathcal{N}(v)}$$

□

A.4 Proposition 3.4

PROOF. According to (4), the variance of $x'_{v,i}$ can be written in terms of the variance of $x^*_{v,i}$ as:

$$\text{Var} [x'_{v,i}] = \left[\frac{d(\beta - \alpha)}{2m} \cdot \frac{e^{\epsilon/m} + 1}{e^{\epsilon/m} - 1} \right]^2 \cdot \text{Var} [x^*_{v,i}]$$

Applying Lemma A.1 yields:

$$\begin{aligned} \text{Var} [x'_{v,i}] &= \left[\frac{d(\beta - \alpha)}{2m} \cdot \frac{e^{\epsilon/m} + 1}{e^{\epsilon/m} - 1} \right]^2 \\ &\quad \times \left(\frac{m}{d} - \left[\frac{m}{d} \cdot \frac{e^{\epsilon/m} - 1}{e^{\epsilon/m} + 1} \cdot \left(2 \cdot \frac{x_{v,i} - \alpha}{\beta - \alpha} - 1 \right) \right]^2 \right) \\ &= \frac{d}{m} \cdot \left(\frac{\beta - \alpha}{2} \cdot \frac{e^{\epsilon/m} + 1}{e^{\epsilon/m} - 1} \right)^2 \\ &\quad - \left[\frac{\beta - \alpha}{2} \cdot \left(2 \cdot \frac{x_{v,i} - \alpha}{\beta - \alpha} - 1 \right) \right]^2 \\ &= \frac{d}{m} \cdot \left(\frac{\beta - \alpha}{2} \cdot \frac{e^{\epsilon/m} + 1}{e^{\epsilon/m} - 1} \right)^2 - \left(x_{v,i} - \frac{\alpha + \beta}{2} \right)^2 \end{aligned}$$

□

A.5 Proposition 3.5

PROOF. We look for a value of m that minimizes the variance of the estimator defined by (4), i.e., $\text{Var}[x'_{v,i}]$, for any arbitrary node $v \in \mathcal{V}$ and any arbitrary dimension $i \in \{1, 2, \dots, d\}$. However, based on Proposition 3.4, $\text{Var}[x'_{v,i}]$ depends on the private feature $x_{v,i}$, which is unknown to the server. Therefore, we find the optimal m , denoted by m^* , by minimizing the upperbound of the variance:

$$m^* = \arg \min_m \max_x \text{Var}[x'] \quad (24)$$

where we omitted the node v and dimension i subscripts for simplicity. From Proposition 3.4, it can be easily seen that the variance is maximized when $x = \frac{\alpha + \beta}{2}$, which yields:

$$\max_x \text{Var}[x'] = \frac{d}{m} \cdot \left(\frac{\beta - \alpha}{2} \cdot \frac{e^{\epsilon/m} + 1}{e^{\epsilon/m} - 1} \right)^2 \quad (25)$$

$$= C \cdot z \cdot \left(\frac{e^z + 1}{e^z - 1} \right)^2 = C \cdot z \cdot \coth^2\left(\frac{z}{2}\right) \quad (26)$$

where we set $z = \frac{\epsilon}{m}$ and $C = \frac{d}{\epsilon} \cdot \left(\frac{\beta - \alpha}{2} \right)^2$, and $\coth(\cdot)$ is the hyperbolic cotangent. Therefore, minimizing (25) with respect to m is equivalent to minimizing (26) with respect to z , and then recover m^* as $\frac{\epsilon}{z^*}$, where z^* is the optimal z minimizing (26). More formally:

$$\begin{aligned} z^* &= \arg \min_z \left[C \cdot z \cdot \coth^2\left(\frac{z}{2}\right) \right] \\ &= \arg \min_z \left[z \cdot \coth^2\left(\frac{z}{2}\right) \right] \end{aligned}$$

where the constant C were dropped as it does not depend on z . The function $f(z) = z \cdot \coth^2(\frac{z}{2})$ is a convex function with a single

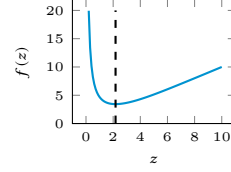


Figure 4: Plotting $f(z) = z \cdot \coth^2(\frac{z}{2})$. The gray dashed line indicate the location of the minimum.

minimum on $(0, \infty)$, as shown in Figure 4. Taking the derivative of $f(\cdot)$ with respect to z and set it to zero gives us the minimum:

$$f'(z) = \frac{d}{dz} z \cdot \coth^2\left(\frac{z}{2}\right) = \coth\left(\frac{z}{2}\right) \left[\coth\left(\frac{z}{2}\right) - z \cdot \text{csch}^2\left(\frac{z}{2}\right) \right] = 0$$

and then we have:

$$z = \frac{\coth(\frac{z}{2})}{\text{csch}^2(\frac{z}{2})} = \frac{\sinh(z)}{2} \quad (27)$$

Solving the above equation yields $z^* \approx 2.18$, and therefore we have $m^* = \frac{\epsilon}{2.18}$. However, m should be an integer value between 1 and d . To enforce this, we set:

$$m^* = \max(1, \min(d, \lfloor \frac{\epsilon}{2.18} \rfloor)) \quad (28)$$

□

A.6 Proposition 3.6

PROOF. According to (4) and depending on Algorithm 1's output, for any node $u \in \mathcal{V}$ and any dimension $i \in \{1, 2, \dots, d\}$, we have:

$$x'_{u,i} = \begin{cases} \frac{\alpha + \beta}{2} - \frac{d(\beta - \alpha)}{2m} \cdot \frac{e^{\epsilon/m} + 1}{e^{\epsilon/m} - 1} & \text{if } x^*_{u,i} = -1 \\ \frac{\alpha + \beta}{2} & \text{if } x^*_{u,i} = 0 \\ \frac{\alpha + \beta}{2} + \frac{d(\beta - \alpha)}{2m} \cdot \frac{e^{\epsilon/m} + 1}{e^{\epsilon/m} - 1} & \text{if } x^*_{u,i} = 1 \end{cases}$$

and therefore

$$x'_{u,i} \in \left[\frac{\alpha + \beta}{2} - C, \frac{\alpha + \beta}{2} + C \right]$$

where

$$C = \frac{d(\beta - \alpha)}{2m} \cdot \frac{e^{\epsilon/m} + 1}{e^{\epsilon/m} - 1} \quad (29)$$

Therefore, considering that $x_{u,i} \in [\alpha, \beta]$, we get:

$$\left| x'_{u,i} - x_{u,i} \right| \leq \frac{\beta - \alpha}{2} + C \quad (30)$$

and also by Proposition 3.2, we know that

$$\mathbb{E} [x'_{u,i} - x_{u,i}] = 0 \quad (31)$$

On the other hand, using the mean aggregator function, for any node $v \in \mathcal{V}$ and any dimension $i \in \{1, 2, \dots, d\}$, we have:

$$\begin{aligned} (h_{\mathcal{N}(v)})_i &= \frac{1}{|\mathcal{N}(v)|} \sum_{u \in \mathcal{N}(v)} x_{u,i} \\ (\widehat{h}_{\mathcal{N}(v)})_i &= \frac{1}{|\mathcal{N}(v)|} \sum_{u \in \mathcal{N}(v)} x'_{u,i} \end{aligned} \quad (32)$$

Considering 30 to 32 and using the Bernstein inequality, we have:

$$\begin{aligned}
 & \Pr \left[\left| (\widehat{h}_{\mathcal{N}(v)})_i - (h_{\mathcal{N}(v)})_i \right| \geq \lambda \right] \\
 &= \Pr \left[\left| \sum_{u \in \mathcal{N}(v)} (x'_{u,i} - x_{u,i}) \right| \geq \lambda |\mathcal{N}(v)| \right] \\
 &\leq 2 \cdot \exp \left\{ - \frac{\lambda^2 |\mathcal{N}(v)|}{\frac{2}{|\mathcal{N}(v)|} \sum_{u \in \mathcal{N}(v)} \text{Var}[x'_{u,i} - x_{u,i}] + \frac{2}{3} \lambda \left(\frac{\beta - \alpha}{2} + C \right)} \right\} \\
 &= 2 \cdot \exp \left\{ - \frac{\lambda^2 |\mathcal{N}(v)|}{2 \text{Var}[x'_{u,i}] + \frac{2}{3} \lambda \left(\frac{\beta - \alpha}{2} + C \right)} \right\} \quad (33)
 \end{aligned}$$

We can rewrite the variance of $x'_{u,i}$ in terms of C as:

$$\text{Var}[x'_{u,i}] = \frac{m}{d} C^2 - \left(x_{v,i} - \frac{\alpha + \beta}{2} \right)^2 \quad (34)$$

The asymptotic expressions involving ϵ are evaluated in $\epsilon \rightarrow 0$, which yields:

$$C = \frac{d(\beta - \alpha)}{2m} \mathcal{O}\left(\frac{m}{\epsilon}\right) = \mathcal{O}\left(\frac{d}{\epsilon}\right) \quad (35)$$

and therefore we have:

$$\text{Var}[x'_{u,i}] = \frac{m}{d} \left(\mathcal{O}\left(\frac{d}{\epsilon}\right) \right)^2 - \left(x_{v,i} - \frac{\alpha + \beta}{2} \right)^2 = \mathcal{O}\left(\frac{md}{\epsilon^2}\right) \quad (36)$$

Substituting (35) and (36) in (33), we have:

$$\Pr \left[\left| (\widehat{h}_{\mathcal{N}(v)})_i - (h_{\mathcal{N}(v)})_i \right| \geq \lambda \right] \leq 2 \cdot \exp \left\{ - \frac{\lambda^2 |\mathcal{N}(v)|}{\mathcal{O}\left(\frac{md}{\epsilon^2}\right) + \lambda \mathcal{O}\left(\frac{d}{\epsilon}\right)} \right\}$$

According to the union bound, we have:

$$\begin{aligned}
 & \Pr \left[\max_{i \in \{1, \dots, d\}} \left| (\widehat{h}_{\mathcal{N}(v)})_i - (h_{\mathcal{N}(v)})_i \right| \geq \lambda \right] \\
 &= \bigcup_{i=1}^d \Pr \left[\left| (\widehat{h}_{\mathcal{N}(v)})_i - (h_{\mathcal{N}(v)})_i \right| \geq \lambda \right] \\
 &\leq \sum_{i=1}^d \Pr \left[\left| (\widehat{h}_{\mathcal{N}(v)})_i - (h_{\mathcal{N}(v)})_i \right| \geq \lambda \right] \\
 &= 2d \cdot \exp \left\{ - \frac{\lambda^2 |\mathcal{N}(v)|}{\mathcal{O}\left(\frac{md}{\epsilon^2}\right) + \lambda \mathcal{O}\left(\frac{d}{\epsilon}\right)} \right\}
 \end{aligned}$$

To ensure that $\max_{i \in \{1, \dots, d\}} \left| (\widehat{h}_{\mathcal{N}(v)})_i - (h_{\mathcal{N}(v)})_i \right| < \lambda$ holds with at least $1 - \delta$ probability, it is sufficient to set

$$\delta = 2d \cdot \exp \left\{ - \frac{\lambda^2 |\mathcal{N}(v)|}{\mathcal{O}\left(\frac{md}{\epsilon^2}\right) + \lambda \mathcal{O}\left(\frac{d}{\epsilon}\right)} \right\} \quad (37)$$

Solving the above for λ , we get:

$$\lambda = \mathcal{O} \left(\frac{\sqrt{d \log(d/\delta)}}{\epsilon \sqrt{|\mathcal{N}(v)|}} \right) \quad (38)$$

□

A.7 Corollary 3.7

PROOF. The forward and backward propagation steps in Algorithm 3.1 only process the output of the multi-bit mechanism, which provides ϵ -LDP for each node based on Theorem 3.1, and private node features are not used anywhere else in the algorithm except by the multi-bit mechanism. Since Algorithm 3 calls the multi-bit mechanism only once per node, and due to the robustness of differentially private algorithms to post-processing [10], Algorithm 3 satisfies ϵ -LDP for each node. □